¹³C and ²³Na Solid-State NMR Study on Zeolite Y Loaded with Mo(CO)₆

Hubert Koller,†,‡ Arian R. Overweg,† Rutger A. van Santen,† and Jan W. de Haan*,‡

Laboratories of Inorganic Chemistry and Catalysis and of Instrumental Analysis, Eindhoven University of Technology, P.O. Box 513, 5600 MB Eindhoven, The Netherlands

Received: September 11, 1996; In Final Form: December 19, 1996[®]

The 23 Na MAS and double rotation (DOR) NMR spectra of dehydrated zeolite NaY loaded with two molecules of Mo(CO)₆ per supercage show three components distinguished by the corresponding quadrupole coupling constants (QCC). Sodium cations in the hexagonal prisms (SI sites) are characterized by a narrow Gaussian line with a QCC value close to zero. A second component with quadrupole coupling constants between 4.4 and 4.8 MHz is assigned to Na⁺ cations located in the sodalite cages, and the third component with QCC ranging between 2.2 and 2.8 MHz is due to sodium cations in the supercages interacting with Mo(CO)₆. These sites are characterized by structural and/or dynamical disorder as observed by typical line shape properties. Adsorption of Mo(CO)₆ in Y zeolites, where all Na⁺ cations in the supercages of NaY have been exchanged with NH₄⁺ or H⁺, causes the sodium cations in the sodalite cages to migrate into the supercages in order to interact with the adsorbent. For the NH₄⁺-exchanged sample, the anisotropic chemical shift parameters for 13 C in Mo(CO)₆ have been analyzed at ambient temperature. From the results a fast anisotropic local reorientation of Mo(CO)₆ follows. The rotation is about a 3-fold axis of the octahedral complex. The octahedron is slightly elongated along the rotation axis by about 4° when it is located close to the sodium cations.

Introduction

Composites of zeolites and transition metal compounds have enjoyed a rising popularity lately. 1-3 This trend is driven by prospects of potential applications for electronic devices, as optical materials, and in heterogeneous catalysis. One possible use of zeolite NaY loaded with Mo(CO)₆ is as a precursor to hydrodesulfurization catalysts. To pursue the ultimate goal of creating 'materials by design', a fundamental knowledge of molecular interactions and mechanisms is in demand. Several questions as to the location, and the dynamics, of Mo(CO)₆ interacting with Na⁺ cations in NaY have been raised.

The cation positions of interest in the structure of zeolite Y are shown in Figure 1. Due to its size, $Mo(CO)_6$ can only enter the supercages in the pore system of zeolite Y (Figure 1). Although several authors have referred to the supercage of the Faujasite structure (Figure 2) as an ' α -cage', this is in fact incorrect. The large void in zeolite A, which is different from the supercage in zeolite Y, is correctly called an α -cage.⁵

The interaction between $Mo(CO)_6$ and the sodium cations in zeolite Y can be studied by ^{23}Na NMR spectroscopy. However, the literature is still inconsistent as to the number and the assignment of lines concerning the ^{23}Na NMR characterization of the unloaded, dehydrated NaY structure. $^{6-8}$

Engelhardt and co-workers have found four components in the ²³Na NMR spectra (MAS, DOR, and two-dimensional MAS nutation) of dehydrated zeolite NaY.⁶ A narrow line with a quadrupole coupling constant (QCC) which is close or equal to zero was assigned to sodium cations in the hexagonal prisms (SI sites, here referred to as component A). A second component (component B) with a quadrupole coupling constant of 4.0 MHz was assigned to sodium on SII sites, and the third line (component C) for SI' is characterized by a QCC value of 4.8 MHz. Another line with a Gaussian/Lorentzian shape

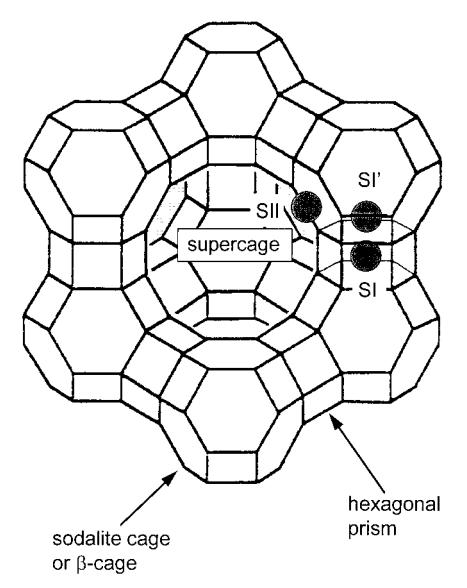


Figure 1. Cation positions in the structure of zeolite Y.

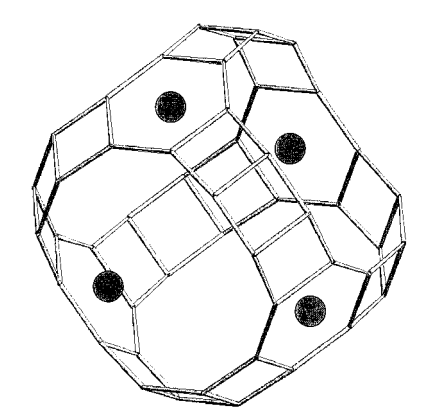


Figure 2. The four SII positions in the supercage of zeolite Y.

centered at -26 ppm ($B_0 = 9.4$ T) has been observed for partially rehydrated Na⁺ cations (component D). These assignments were derived by calculations of electric field gradients

^{*} Author to whom all correspondence should be addressed. Tel.: (+31) 40 247 3022. FAX: (+31) 40 245 3762.

[†] Laboratory of Inorganic Chemistry and Catalysis.

Laboratory of Instrumental Analysis.

[⊗] Abstract published in Advance ACS Abstracts, February 1, 1997.

for the different sites with a point charge model⁹ and by ion exchanged samples.¹⁰ For a cesium-exchanged zeolite Y, the results from NMR are confirmed by a Rietveld refinement.¹¹ In a recent study, these results are further corroborated by varying the Si/Al ratio, i.e., a series of NaY and NaX zeolites has been studied.¹²

Seidel and Boddenberg only distinguished between two components in the ²³Na MAS NMR spectrum of dehydrated NaY.⁷ Components B and C were observed as one sole component besides A, while D was not found. The interpretation of the lines observed by Seidel and Boddenberg is consistent with ref 6.

The number of components in the ²³Na NMR spectra of dehydrated zeolite NaY in ref 6 is consistent with the results of Verhulst et al.⁸ However, the assignment to sodium positions in ref 8 is in part different from the one described above. Particularly, component C was attributed to sodium cations at SIII positions, and component D has been assigned to the sodium cations in the sodalite cages (SI' and SII'); components A and B were interpreted as in refs 6 and 7. The alternative assignments of lines C and D were based on far-infrared spectroscopic experiments and on ²³Na NMR studies with samples loaded with Mo(CO)₆. The assignment of the bands in far-infrared spectra to distinct cation positions in zeolite Y¹³ being invoked in ref 8 has been questioned recently.¹⁴ We therefore feel that, under these new circumstances, far-infrared band assignments should not be used at this point in time to unravel the problems with inconsistent ²³Na NMR line interpretations. This latest knowledge has triggered in our laboratories a reconsideration of the ²³Na NMR spectra of dehydrated NaY in concert with a deeper study of NaY loaded with Mo- $(CO)_6$.

²³Na double rotation (DOR) NMR investigations on NaY zeolites loaded with Mo(CO)₆ have been published by Jelinek, Ozin, and co-workers^{15–17} and by Verhulst et al.⁸ The spectra of Jelinek show poor resolution. Nevertheless, ²³Na DOR NMR spectra at two different magnetic fields resulted in a quadrupole coupling constant of 2.2 MHz for the sodium cations interacting with the adsorbed complex.¹⁶ Verhulst et al. found a similar value of 2.8 MHz by simulating the ²³Na MAS and DOR NMR spectra at 9.4 T. However, the presence of the expected ²³Na NMR signal of sodium cations in the sodalite cages remains unclear^{15–17} or its assignment is a matter of the aforementioned discrepancy.^{6–8}

Another question concerns the location of $Mo(CO)_6$ and its orientation toward the sodium cations as well as the ubiquitous possibility of reallocations of extraframework cations upon incorporation of molecules into the supercages of zeolite Y. Infrared spectroscopic experiments indicate that the symmetry of $Mo(CO)_6$ in NaY is C_{2v} or lower. 19,20 On the basis of space-filling models, Ozin's group favors a structure where $Mo(CO)_6$ is sandwiched between two sodium cations in one supercage (see Figure 2) with one CO group interacting with Na⁺ on either side. 17 This means that $Mo(CO)_6$ interacts along its 4-fold symmetry axis with two Na⁺ cations in the supercage. By contrast, Brémard et al. have suggested by using Monte Carlo simulations that the adsorbed molecules are close to the 12-membered ring windows of the supercages at saturation loading. 18

Here, a reconsideration of the ²³Na solid-state NMR data of Mo(CO)₆-loaded NaY is presented in concert with the implications for the unloaded zeolite. ¹³C NMR investigations give evidence of the motional processes and the local symmetry of the metal—carbonyl complexes. The motion and the local symmetry of Mo(CO)₆ are expected to depend on the nature of

extraframework cations. To this end, the cations in the supercages of zeolite Y were varied by exchanging H^+ or NH_4^+ for Na^+ cations.

Experimental Section

Sample Preparation. Zeolite NaY was obtained from Akzo Chemicals, and its unit cell composition in dehydrated notation is Na₅₅(AlO₂)₅₅(SiO₂)₁₃₇. For dehydration, ca. 1 g of the asreceived powder was filled into glass ampoules of 12 mm outer diameter. The bed of about 4 cm in height was evacuated overnight, then warmed to 323 K for 2 h while continuously pulling vacuum, and finally the temperature was raised to 723 K and maintained for another 5 h. Afterward, the ampoules were cooled down to room temperature and flame-sealed under vacuum until use. Ammonium exchange was carried out at 353 K with a 1 M solution of NH₄Cl. The zeolite powder was subsequently washed with copious amounts of water. The sodium content remaining in the zeolite was analyzed with atomic absorption spectrometry. One exchange cycle gave a sample with 70% NH₄ exchanged for sodium, and higher exchanged zeolites were obtained by repeating the procedure several times. The dehydration of the Na,NH₄-Y samples was achieved by ramping the temperature with a rate of 2 K/min first to 353 K and then to 433 K, and holding both steps for 2 h. For deammoniation, the temperature was raised to 723 K and maintained for 12 h. All steps were carried out under dynamic vacuum; the final pressure was lower than 10^{-4} mbar for all samples. Rehydration and decomposition of the structures can be excluded on the basis of ¹H MAS NMR control experiments.

Loading experiments were performed under nitrogen in a glovebox by gravimetrically combining the dehydrated zeolite powder and Mo(CO)₆ in a glass ampoule which was then sealed and heated to typically 383 K. The designation xMo(CO)₆/NaY indicates the average number x of Mo(CO)₆ molecules per supercage. If the combined solids (NaY and Mo(CO)₆) were ground in a mortar in the glovebox, then intracage adsorption and partial decarbonylation started within minutes. This decomposition reaction was discerned by a yellow color.²² In the sealed glass tubes, however, this decomposition of the carbonyl complexes was efficiently suppressed, even at temperatures as high as 423 K.

NMR Experiments. ¹H, ¹³C, and ²³Na MAS NMR experiments were obtained with a Bruker MSL-400 spectrometer operating at a magnetic field of $B_0 = 9.4$ T. Selected ²³Na MAS NMR spectra were also acquired on AM-500 and AMX-600 spectrometers operating with magnetic fields of $B_0 = 11.7$ and 14.1 T, respectively. Chemical shifts are relative to TMS (1H and 13C MAS NMR) and to solid NaCl (23Na MAS NMR). Standard Bruker MAS probe heads have been used for the experiments with ¹³C (7 mm rotor diameter, spinning speed up to 3.5 kHz) and ¹H, ²³Na (4 mm rotor diameter, spinning speed up to 15 kHz). ²³Na MAS NMR spectra on the AM-500 and AMX-600 spectrometers were acquired at the University of Nijmegen with a spinning speed of ca. 13 kHz using a homemade probe head. Static ¹³C NMR spectra were also obtained with a static probe head in glass containers of 1 cm diameter.

The ²³Na DOR NMR experiments were obtained using a commercial probe head, as delivered by Bruker, operating with up to a 1000 Hz spinning speed of the outer rotor. The rotor—synchronized pulse method of Samoson and Lippmaa²¹ was applied in order to remove the odd-numbered spinning sidebands of the outer rotor. Center lines were distinguished from spinning sidebands by varying the spinning frequency of the outer rotor. The empty DOR rotors were stored at least for one day in a

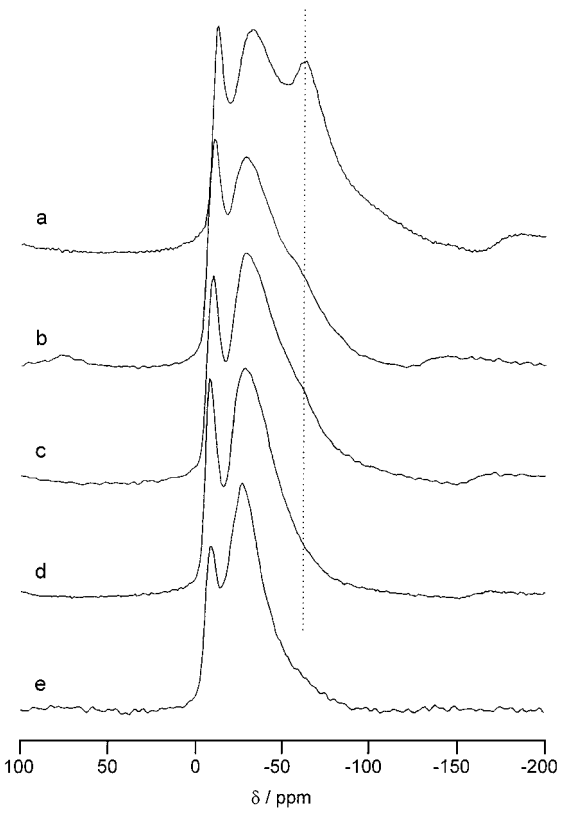


Figure 3. ²³Na MAS NMR spectra of (a) dehydrated NaY, (b) a physical 1:1 mixture of dehydrated NaY and 2Mo(CO)₆/NaY, (c) 1.4Mo(CO)₆/NaY, (d) 2Mo(CO)₆/NaY, and (e) NaY saturated with Mo(CO)₆ in a helium flow.

dry glovebox and filled directly before the experiment. Control experiments showed that the dry zeolite adsorbs water from the rotors if this precaution has not been taken.

Simulations of the DOR NMR experiments were carried out with the program QNMR (A. Samoson, Tallin, Estonia), and MAS NMR spectra were analyzed with the WINFIT software (Bruker, Rheinstetten, Germany).

Results

²³Na NMR of Dehydrated NaY. The difference between the ²³Na NMR spectra of different research groups^{6–8} has been reexamined by comparing the different dehydration techniques applied. It turned out that drying the NaY sample in a He flow at a maximum temperature of 673 K did reproduce the ²³Na NMR features presented in ref 8, i.e., component D showed substantial intensity. However, on the basis of ¹H MAS NMR experiments, trace amounts of silanol groups were observed in this sample. In contrast, these silanol group signals are much reduced, and the intensity of component D has disappeared in the ²³Na MAS NMR spectrum, when the zeolites are dehydrated under vacuum without exposition to a helium flow. The ²³Na NMR spectra are then consistent with the result in ref 6. It is not clear whether the difference is caused by the variant pressure and atmospheric conditions for dehydration, or by the modified heating regimes of the samples in refs 6,8. Additionally, crosschecking experiments of NaY samples with the group of the University of Stuttgart, Germany (G. Engelhardt and M. Hunger) made us feel more confident with the vacuum dehydration technique. Accordingly, the ²³Na NMR assignments of lines A, B, and C are adopted from ref 6.

²³Na NMR of NaY Loaded With Mo(CO)₆. Figure 3 shows a collection of ²³Na MAS NMR spectra of dehydrated NaY (Figure 3a) and Mo(CO)₆-loaded NaY samples (Figure 3b—e).

Figure 3b shows the result obtained on a 1:1 physical mixture of dehydrated NaY and 2Mo(CO)6/NaY, Figure 3c is from 1.4Mo(CO)₆/NaY, and Figure 3d shows the ²³Na MAS NMR spectrum of 2Mo(CO)₆/NaY, the latter corresponding to saturation loading.²² All these samples were prepared as outlined in the experimental section. By contrast, the experiment which is displayed in Figure 3e is from a NaY sample that has been dehydrated and saturated with Mo(CO)₆ in a He flow at 333 K according to the procedure described in ref 8. This spectrum is clearly different from Figure 3d and rather equals the result shown in ref 8. The relative peak heights are different in Figures 3d,e, and the positions of the lines at high field are -29 ppm in Figure 3d and -19 ppm in Figure 3e. The color of the sample represented by its ²³Na MAS NMR spectrum in Figure 3e was dark yellow due to an unknown amount of decarbonylated species. For this reason, and because of the aforementioned concerns with the helium flow technique, we will focus on the samples which were made without exposing them to a He flow (Figures 3, lines a-d).

Loadings which are nominally higher than two molecules per supercage yielded ²³Na MAS NMR spectra that are indistinguishable from the result shown in Figure 3d. This observation is expected, since the maximum loading of the supercages in NaY with Mo(CO)₆ is achieved with about two molecules.²² Various annealing temperatures between 293 and 423 K of the ampoules with the 2Mo(CO)₆/NaY mixture did not give any results different from Figure 3d either. Obviously, the uptake of Mo(CO)₆ vapor in the zeolite pores is easily accomplished by mixing at room temperature and the distribution of the molecules in the supercages reaches equilibrium in a short time (less than 1 day based on changes in ²³Na MAS NMR spectra).

The sharp peak in Figure 3a at ca. -10 ppm is from sodium cations in the hexagonal prisms of dehydrated NaY. These sites are in a fairly symmetric environment which results in a quadrupole coupling constant for 23 Na which is close to zero. This line does not change upon loading. The two maxima on the upfield side in Figure 3a are in the range (ca. -20 to -150 ppm, $B_0 = 9.4$ T) where the two quadrupole components for sodium cations in the sodalite and supercages have been found in NaY.⁶ The dotted line in Figure 3 is placed on the right singularity of the quadrupole component originating from sodium cations in the supercages at SII positions. The disappearence of this feature in Figure 3 is obvious when the loading with Mo(CO)₆ is increased.

The MAS technique appears to be an appropriate method for the preliminary purpose to characterize the progress of pore filling. However, for a more sophisticated analysis of the ²³Na NMR components, a combination of several methods is needed. Due to the large quadrupole interaction of the sodium cations in the supercages and sodalite cages of NaY,⁶ the new triple-quantum method for line narrowing²³ did not prove usefull. This is consistent with the predicted limitation of this method to QCC values of 4 MHz or less.²³

On the basis of the electric field gradient calculations,⁹ an increase of the coordination number of a sodium cation at SII would decrease the quadrupole coupling constant of ²³Na.²⁴ This prediction has been confirmed experimentally for the interaction with meta-xylene molecules,²⁵ and as will be shown below by a combination of ²³Na MAS and DOR NMR experiments, it will hold true for Mo(CO)₆ in a deeper analysis of the experiment displayed in Figure 3d.

Figure 4 shows the ²³Na MAS and DOR NMR experiments of 2Mo(CO)₆/NaY in parts a and c, respectively. The sharp signal at 0 ppm in Figure 4c is from a small NaCl impurity in the DOR rotor which serves for chemical shift calibration. The

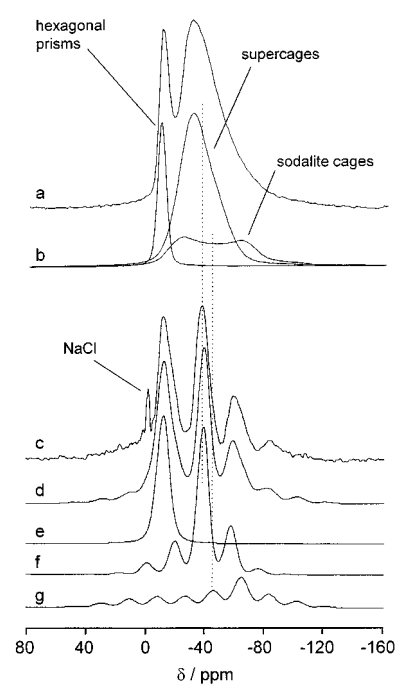


Figure 4. (a) ²³Na MAS NMR spectrum of 2Mo(CO)₆/NaY; (b) components of (a); (c) ²³Na DOR NMR spectrum of 2Mo(CO)₆/NaY; (d) simulation of components e−g, (e) Gaussian line at −9.9 ppm; (f) quadrupolar component with QCC = 2.8 MHz, η = 0.4, and $\delta_{\rm iso}$ = -19.7 ppm; (g) quadrupolar component with QCC = 4.4 MHz, η = 0.2, and $\delta_{iso} = -1.6$ ppm.

Gaussian component at -9.9 ppm in Figure 4e is readily assigned to sodium cations in the hexagonal prisms.^{6–8} The corresponding component for the MAS NMR experiment is shown in Figure 4b. This line does not show any spinning sidebands. Another center line in Figure 4c is at -36.2 ppm, and all other maxima are due to spinning sidebands. The distance in Figure 4c between the maxima at -36.2 and -58.8ppm is ca. 2400 Hz. This number is inconsistent with the applied spinning speed of 1000 Hz of the outer rotor if the maximum at -58.8 ppm would be due to one spinning sideband only. Instead, a difference of 2000 Hz is expected, i.e., twice the value of the physical spinning speed because of the elimination of the odd-numbered spinning sidebands. It must follow that at least two components contribute to the maxima at -36.2 and -58.8 ppm in Figure 4c. The asymmetric shape of the spinning sideband with its maximum at -58.8 ppm supports this conclusion. Therefore, the two quadrupolar lines which are shown in Figures 4f,g were included into the ²³Na DOR NMR analysis of 2Mo(CO)₆/NaY. Their centers are indicated by dotted lines in Figure 4. The component in Figure 4f is characterized by a QCC value of 2.8 MHz, an asymmetry parameter of $\eta = 0.4$, and a chemical shift (δ_{iso}) of -19.7 ppm. Figure 4g was generated by the fit values QCC = 4.4 MHz, η = 0.2, and δ_{iso} = -1.6 ppm. The large quadrupole coupling constant of the latter component is expected for sodium cations in the sodalite cages according to ref 6, where a value of 4.8 MHz has been reported for unloaded NaY. The corresponding MAS NMR component for the sodium cations in the sodalite cages (Figure 4b) exhibits the typical quadrupolar line shape. As a consequence of the lines assigned so far, the central component with QCC = 2.8 MHz (Figure 4f) is attributed to Na⁺ cations in the supercages which interact with Mo(CO)₆ molecules.

The shape of the corresponding MAS NMR component does not show the usual quadrupolar characteristics (Figure 4b). It was fitted by two ordinary Gaussian lines which form an

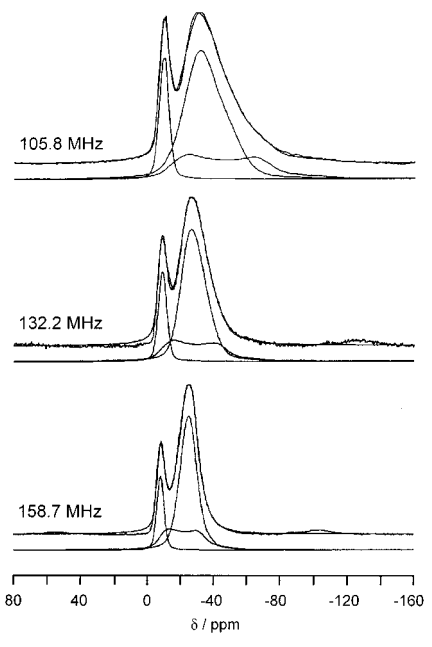


Figure 5. ²³Na MAS NMR spectra and simulations (upper traces) for 2Mo(CO)6/NaY and the individual components (lower traces) for the three indicated resonance frequencies.

asymmetric peak (Figure 4b) whose center of gravity is consistent with the position of the DOR NMR component in Figure 4f. This kind of MAS NMR line shape of quadrupole nuclei is typical for sites that are structurally or dynamically disordered.²⁶ The quadrupolar features in these lines are smeared by a distribution of line shape parameters (QCC, η , and $\delta_{\rm iso}$). Here, only the average values of the parameters can

The analysis of the ²³Na MAS NMR spectrum of 2Mo(CO)₆/ NaY is further confirmed at higher magnetic fields ($B_0 = 11.7$ and 14.1 T), and the results are shown in Figure 5. For each field, the lower traces show the three simulated components, and the two upper traces are the experimental and the simulated spectrum. The position of the Gaussian component at -9.9ppm is not altered upon changing the magnetic field, and the quadrupolar component for Na⁺ in the sodalite cages is simulated with the above values for QCC (4.4 MHz), η (0.2), and $\delta_{\rm iso}$ (-1.6 ppm) for all three fields. As described above for the 105.8 MHz spectrum, the remaining central part of the spectrum was simulated with two Gaussian lines which are combined to one component in Figure 5. The decrease of the broadness and of the asymmetry of this latter component upon increasing the magnetic field (Figure 5) confirms that it is a quadrupolar line typical for disordered systems.

The dependence on the magnetic field strength of the center of gravity (δ_{cg}) of the asymmetric line for the sodium cations in the supercages has been analyzed in Figure 6. δ_{cg} is plotted as a function of $1/\nu_L^2$, ν_L being the Larmor frequency for ²³Na. A linear correlation is found in Figure 6 according to the equation

$$\delta_{\rm cg} = \delta_{\rm iso} - \frac{10^6}{40} \frac{\rm QCC^2}{\nu_{\rm L}^2} \left(1 + \frac{\eta^2}{3}\right)$$
 (1)

This method readily yields the isotropic chemical shift of -19.0 ppm which is in very good agreement with the value of -19.7 ppm obtained from the DOR NMR simulation. The quadrupole coupling constant as derived from the slope of the linear correlation in Figure 6 is 2.6 MHz if an asymmetry parameter of $\eta = 0$ is assumed. Changing η to 0.4, viz., the

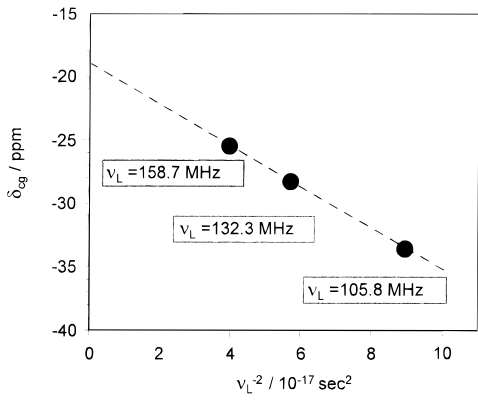


Figure 6. Center of gravity of the asymmetric central component in Figure 5 (see text) as a function of $1/\nu_L^2$.

TABLE 1: Quadrupole Interaction Parameters and Chemical Shifts for ²³Na in Dehydrated Zeolite NaY (Values from ref 6) and NaY Loaded with Two Mo(CO)₆ Molecules per Supercage

	QCC/MHz	η	$\delta_{ m iso}$ /ppm
dehydrated NaY			
SI	ca. 0.1	0	-11.8
SI'	4.8	0.2	-3.5
SII	4.0	0.2	-11.8
2Mo(CO) ₆ /NaY			
SI	ca. 0	nd^a	-9.9
SI'	4.4 - 4.8	0.2	-1.6
SII	2.2 - 2.8	0.4	-19.7

a nd = no data.

value obtained by the DOR NMR simulation, leads to a QCC value of 2.5 MHz and for $\eta=1.0$ a value of 2.2 MHz is obtained. These values of QCC as derived from this analysis are reasonably close to the result from the DOR NMR simulation (2.8 MHz). Due to the overlap of components in the ²³Na NMR spectra of 2Mo(CO)₆/NaY, and because of the disorder, a slight variation of QCC values must be considered. On the basis of the combination of methods as described above, a range between 2.2 and 2.8 MHz for the central component for Na⁺ in the supercages can be given with confidence. Several simulation models have been tested, and the results being consistent with all ²³Na MAS and DOR NMR experiments are listed in Table 1. The quantitative analysis (not shown) of the components in the ²³Na MAS and DOR NMR spectra of $2\text{Mo}(\text{CO})_6/\text{NaY}$ does not show that Na⁺ migrates upon Mo(CO)₆ adsorption.

Ion Exchange with NH₄⁺ and H⁺. Further results on the dynamics of Mo(CO)₆ were obtained with NH₄⁺-exchanged samples and their deammoniated H-forms. Figure 7 shows the ¹H MAS NMR spectra of unloaded (Figures 7a,c) and loaded (Figures 7b,d) Na,NH₄-Y (Figures 7a,b) and Na,H-Y (Figures 7c,d). Seventy percent of NH₄⁺ or H⁺ ions are exchanged for Na⁺. The corresponding ²³Na MAS NMR spectra of these samples are shown in Figure 8. Dehydrated Na,NH₄-Y shows a proton MAS NMR signal at 6.8 ppm for ammonium cations in the supercages (Figure 7a). A small portion of ammonium cations has been decomposed, giving rise to the signals for acid sites between 3 and 4.5 ppm in the ¹H MAS NMR spectrum. Surprisingly, the NH₄⁺ signal at 6.8 ppm shifts slightly to 6.5 ppm upon adsorption of Mo(CO)₆. This effect will be discussed in conjunction with Figure 8. The ¹H MAS NMR spectrum of the Na,H-Y sample in Figure 7c shows a maximum at 3.7 ppm for Brønsted protons in the supercages and a shoulder at 4.5 ppm for protons in the sodalites cages. After adsorption of Mo-(CO)₆, only one peak centered at 4.5 ppm can be identified. Obviously, the proton NMR signal at 3.7 ppm shifts to lower

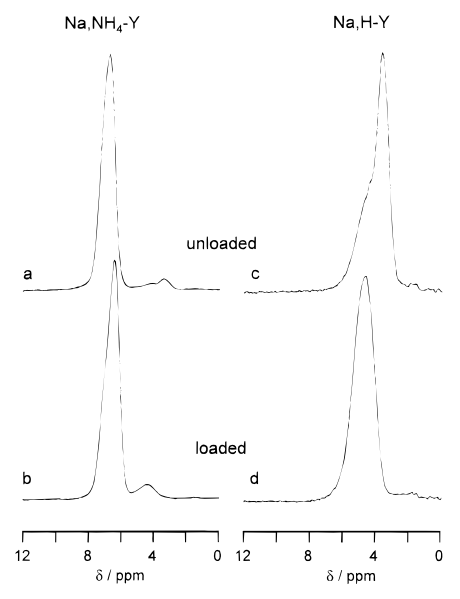


Figure 7. ¹H MAS NMR spectra of (a) Na,NH₄-Y, (b) 2Mo(CO)₆/Na,NH₄-Y, (c) Na,H-Y, and (d) 2Mo(CO)₆/Na,H-Y.

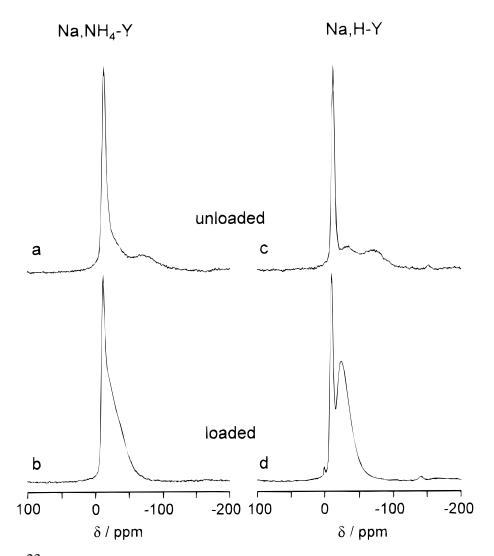


Figure 8. ²³Na MAS NMR spectra of (a) Na,NH₄-Y, (b) 2Mo(CO)₆/Na,NH₄-Y, (c) Na,H-Y, and (d) 2Mo(CO)₆/Na,H-Y.

field upon interaction of the Brønsted sites in the supercages with Mo(CO)₆, and it then overlaps with the line from protons in the sodalite cages. The observed low-field shift is due to a weak hydrogen bond between the Brønsted protons and the oxygen atoms of the carbonyl groups.

An interesting observation is made in the ²³Na MAS NMR spectra in Figure 8. In Figures 8a,c two components are readily identified. The sharp signals at -12.2 ppm (Figure 8a) or at -11.0 ppm (Figure 8c) originate from Na⁺ cations at SI sites in Na,NH₄-Y or in Na,H-Y, respectively. Deconvolutions of both spectra show that there is a quadrupolar line upfield from this sharp component. Recall that NH₄⁺ or H⁺ have been substituted for 70% of the Na⁺ cations. In a cesium-exchanged sample,¹¹ this quadrupolar line shape was unequivocally attributed to the sodium cations in the sodalite cages by employing a combination of ²³Na MAS NMR spectroscopy and Rietveld refinement. After adsorption of Mo(CO)6, the quadrupolar line shapes have completely disappeared and a Gaussian line is observed instead. This signal is exhibited as a shoulder upfield from the Gaussian line for SI cations in Figure 8b and shows a maximum at -24 ppm in Figure 8d. These drastic changes from quadrupolar to Gaussian lines are a clear indication of

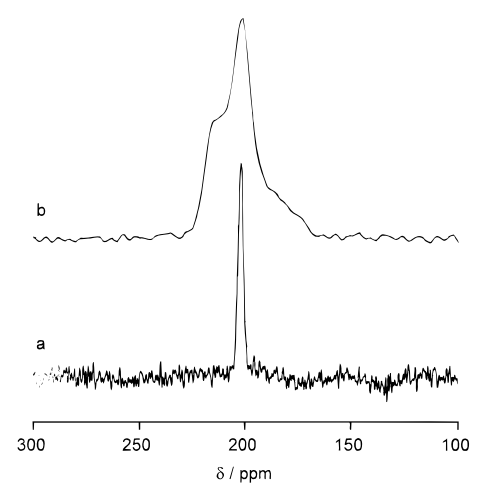


Figure 9. (a) Static ¹³C NMR spectrum of 2Mo(CO)₆/NaY and (b) static ¹³C cross-polarization (CP) NMR spectrum of 2Mo(CO)₆/Na,- NH_4-Y .

migration of the sodium cations of the sodalite cages into the supercages. The corresponding ²³Na MAS NMR line shapes change due to the interaction of Na⁺ with Mo(CO)₆. The shift to higher field of the proton NMR signal for the NH₄⁺ cations as described above is consistent with a counter migration of ammonium cations into the sodalite cages, at least to some extent.²⁷ Note that the samples whose MAS NMR spectra are shown in Figures 7b,d and 8b,d have been annealed at 373 K for 10 h which may have facilitated cation migration. This Na⁺ migration is at a striking difference to the behavior of dehydrated NaY which shows no or only minor Na⁺ cation migrations from the sodalite cages into the supercages upon loading.

Dynamics of Mo(CO)₆. The Mo(CO)₆ molecules exhibit different mobilities in the supercages of NaY, Na,H-Y, and Na,NH₄-Y. These differences are demonstrated by the line narrowing in ¹³C NMR spectra due to the dynamic averaging of chemical shift anisotropy of the carbonyl ligands.²⁸ Figure 9a shows the static ¹³C NMR spectrum of Mo(CO)₆ in zeolite NaY. A relatively sharp line is observed at 202 ppm which is similar to the result obtained on Na,H-Y (not shown). A broader spectrum is shown in Figure 9b for 2Mo(CO)₆/Na,-NH₄-Y. This spectrum was obtained at room temperature using {1H-}13C cross-polarization in order to improve the signal-tonoise ratio. No 13C NMR signals other than the one shown in Figure 9b are observed without cross-polarization, except for a broad probe background. No cross-polarization ¹³C NMR spectrum could be obtained for Mo(CO)₆ in NaY or in Na,H-Y at room temperature. The line width in Figure 9b is analyzed in terms of motional narrowing.

According to the convention introduced in ref 29, the principal values of the chemical shift tensor are $\delta_{11} \ge \delta_{22} \ge \delta_{33}$ and the span Ω is defined for axially symmetric shift tensors (δ_{11} = $\delta_{22} = \delta_{\perp}, \, \delta_{33} = \delta_{||}$ as

$$\Omega = \delta_{\perp} - \delta_{\parallel} \tag{2}$$

In case of rotational motion, the dynamically averaged span is

$$\Omega_{\rm dyn} = \frac{1}{2} (3\cos^2 \Theta - 1) \Omega_{\rm rigid} \tag{3}$$

where Θ is the angle between the rotation axis and the direction of δ_{\parallel} . For octahedral Mo(CO)₆, δ_{\parallel} is in the direction of the collinear Mo–C–O bonds. By measuring Ω_{dyn} and comparing it to the well-known value of $\Omega_{rigid} = 410$ ppm for bulk Mo- $(CO)_{6}$, 30,31 the rotation angle Θ can be estimated. This method has been applied by Oldfield and co-workers to a Mo(CO)5

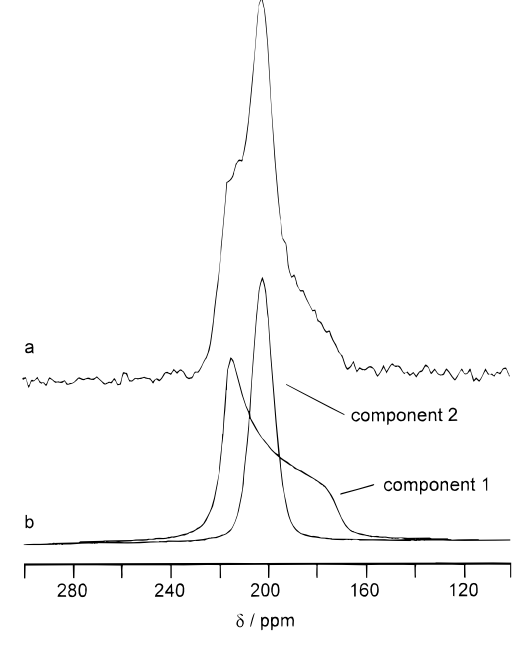


Figure 10. Decomposition of Figure 9b into two components.

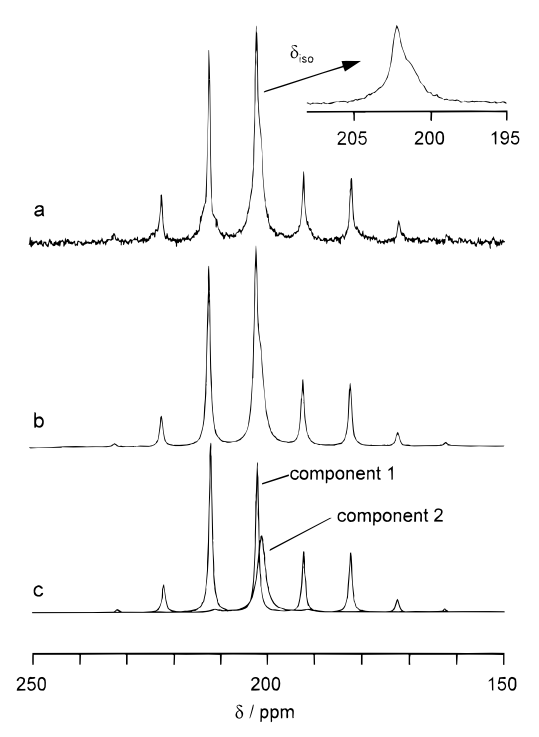


Figure 11. (a) ¹³C CPMAS NMR spectrum of 2Mo(CO)₆/Na,NH₄-Y at 293 K (spinning speed 1 kHz), (b) simulation of the spectrum, and (c) components of the simulation.

fragment which was adsorbed on γ -alumina.³¹ These authors showed, by the reduction of the span Ω by a factor of about -1/2 for four carbonyl ligands, that the rotation angle Θ is ca. 90° according to eq 3, i.e., the rotation is about the 4-fold symmetry axis in that case.

Figure 10a shows the static ¹³C NMR spectrum of 2Mo(CO)₆/ Na,NH₄-Y consisting of the two components shown in Figure 10b. Component 1 is a typical axially symmetric powder pattern for anisotropic chemical shift interaction ($\delta_{iso} = 202.3$ ppm and $\Omega = 45$ ppm). The evidence for this interpretation is given by the ¹³C MAS NMR spectrum (Figure 11), which is discussed below. Component 2 is simulated by a Gaussian line, because it is too narrow and uncharacteristic to extract anisotropic chemical shift parameters. Component 2 grows at the expense of component 1 if the degree of exchange of NH_4^+ for Na^+ cations exceeds 70%.

A confirmation of the analysis of the static ^{13}C NMR spectrum is obtained in Figure 11 by the ^{13}C MAS NMR spectrum with slow rotation (1 kHz). The expansion of the spectrum shown in the inset in Figure 11a clearly confirms the presence of two different lines by a center line at 202.3 ppm and a shoulder at 201.3 ppm. All other lines in Figure 11a are spinning sidebands which are mainly due to component 1. The components are shown in Figure 11c, and the simulation is depicted in Figure 11b. Component 1 in Figure 11c was simulated with the same parameters as those of the chemical shift powder pattern in Figure 10 ($\delta_{\text{iso}} = 202.3$ ppm and $\Omega = 45$ ppm). By eq 3, an angle Θ of 50.4° is obtained for component 1. For component 2, the angle Θ must be close to the magic angle of 54.7°; from the static line width a range between 53 and 56° is estimated.

Discussion

The analysis of ²³Na NMR spectra of dehydrated zeolite NaY samples is another example of the crucial importance of sample preparation techniques. The dehydration of the powders in a helium flow created a small amount of silanol groups as opposed to dehydration under vacuum. This small difference and, perhaps, SiO⁻ Na⁺ defect sites or firmly bound water molecules escaping detection by ¹H NMR cause significant differences in ²³Na MAS and DOR NMR experiments. The difference is an additional component (component D) in the spectra. The results here unequivocally support the interpretation of ²³Na NMR components for dehydrated NaY as suggested in refs 6 and 12.

The quadrupole component in the ²³Na MAS and DOR NMR spectra for Na⁺ cations at SI' suggests that Mo(CO)₆ did not enter the sodalite cages. This is of course expected, because the complex is too bulky for a penetration through the six-ring windows. The displacement of the sodium cations from sodalite cages to supercages for Na,NH₄-Y and Na,H-Y upon adsorption of the hexacarbonyl complex is an indication of a preferred interaction between Mo(CO)₆ and the Na⁺ cations over H⁺ or NH₄⁺. Nevertheless, a weak hydrogen bond interaction is observed between Mo(CO)₆ and the Brønsted acid sites in the supercages. This observation is made by the small low-field shift in the ¹H MAS NMR signal of these sites. On the contrary, no such hydrogen bonding was observed in the proton NMR spectra of the NH₄⁺ cations, since the signal moves slightly upfield upon adsorption of Mo(CO)₆. This shift was explained by a partial displacement of ammonium cations into the sodalite cages as a counter-migration process for the sodium cations displacing from there to the supercages. Nevertheless, Mo(CO)₆ is also in the proximity of residual NH₄⁺ cations in the supercages as suggested by the cross-polarization transfer between the protons of NH₄⁺ and ¹³C in Mo(CO)₆.

In NaY there is a high mobility of the hexacarbonyl complex which is described as liquid-like at room temperature on the basis of ^{95}Mo NMR T_1 relaxation data. 32 Here, the static ^{13}C NMR line at room temperature is narrowed by a completely averaged chemical shift anisotropy of the carbonyl ligands in NaY. The same is true for $2Mo(CO)_6/Na,H-Y$ at room temperature. This isotropic motion consists most likely of local reorientation and diffusion or jump processes between the Na $^+$ and/or H^+ sites in the supercages.

The ¹³C chemical shift anisotropy of Mo(CO)₆ in the supercages of Na,NH₄-Y is rationalized by a local reorientation of the molecule. This motion reduces the line broadening with respect to the static case, but does not average it isotropically in Na,NH₄-Y. The jump rate of Mo(CO)₆ to neighboring sites

must be slow and the local anisotropic reorientation fast on the NMR time scale, which is in the order of 50 kHz given by the static line width for rigid $Mo(CO)_6$.^{30,31} These local reorientations provide an indication as to the local orientation of the $Mo(CO)_6$ complexes towards the sodium cations.

For an ideal Mo(CO)₆ octahedron, the angle between any of the four 3-fold symmetry axes and any of the six C-O bond directions is the magic angle (54.7°). A rotation of an undistorted Mo(CO)₆ molecule about a 3-fold axis would lead to a sharp ¹³C NMR line according to eq 3. Judging from the slight line broadening characterized by a span value of $\Omega = 45$ ppm for component 1 in Figure 10, the rotation deviates by about 4° from the magic angle. The octahedra must be either slightly elongated by this amount or an additional motion of the rotational director by a few degrees is superimposed. From the variation of the ratio of Na⁺ and NH₄⁺ cations, it follows that component 1 is due to Mo(CO)₆ molecules located at sodium cations. It seems likely that the Mo(CO)₆ molecules are sandwiched between two Na⁺ cations along their 3-fold rather than their 4-fold axis in Na,NH₄-Y. For molecules rotating about the 4-fold axis, another component with a span Ω of -205 ppm would be expected. These results show that the model of Ozin¹⁷ for Mo(CO)₆ docking at the sodium sites in NaY cannot explain the interaction between Na⁺ and Mo-(CO)₆ in Na,NH₄-Y. The discrepancy between Brémard¹⁸ and Ozin¹⁷ on the location of the metal complex cannot be solved by the data here. The observation that the narrow component 2 in the ¹³C NMR spectra increases if the substitution of NH₄⁺ for Na⁺ cations increases implies that at least a part of the narrow component corresponds to lesser distorted Mo(CO)₆ in the proximity of NH₄⁺. Further experiments at variable temperatures on the mobility of Mo(CO)6 in NaY and HY zeolites will be published elsewhere.³³

Acknowledgment. This work was funded by the European Union under Contract ERBCHBGCT930309. We gratefully acknowledge the help of G. H. Nachtegaal, University of Nijmegen, at the AM-500 and AMX-600 spectrometers, as well as the multiquantum experiment by S. Steuernagel, Bruker Analytische Messtechnik, Rheinstetten, Germany. Technical support by L. J. M. van de Ven at the MSL-400 spectrometer is highly appreciated. Special thanks are offered to A. Samoson for the latest QNMR version. Finally, we would like to express our appreciation to the colleagues at the University of Stuttgart, Germany (G. Engelhardt, M. Hunger, and M. Feuerstein) for cross-checking samples and for handing out ref 12 prior to publication.

References and Notes

- (1) Ozin, G. A.; Gil, C. Chem. Rev. 1989, 89, 1749.
- (2) Balkus, K. J., Jr.; Gabrielow, A. G. In *Inclusion Chemistry with Zeolites: Nanoscale Materials by Design*; Herron, N., Corbin, D. R., Eds.; Kluwer Academic Publishers: Dordrecht, 1995.
- (3) Van de Goor, G.; Lindlar, B.; Felsche, J.; Behrens, P. *J. Chem. Soc., Chem. Commun.* **1995**, 2559.
- (4) Vorbeck, G.; Welters, W. J. J.; Van de Ven, L. J. M.; Zandbergen, H. W.; De Haan, J. W.; De Beer, V. H. J.; Van Santen, R. A. *Stud. Surf. Sci. Catal.* **1994**, *84*, 1617 and references therein.
- (5) Breck, D. W. Zeolite Molecular Sieves; John Wiley & Sons: New York, 1974.
- (6) Engelhardt, G.; Hunger, M.; Koller, H; Weitkamp, J. Stud. Surf. Sci. Catal. 1994, 84, 421.
 - (7) Seidel, A.; Boddenberg, B. Z. Naturforsch. 1995, 50A, 199.
- (8) Verhulst, H. A. M.; Welters, W. J. J.; Vorbeck, G.; Van de Ven, L. J. M.; De Beer, V. H. J.; Van Santen, R. A.; De Haan, J. W. J. Phys. Chem. **1994**, *98*, 7056.
- (9) Koller, H.; Engelhardt, G.; Kentgens, A. P. M.; Sauer, J. J. Phys. Chem. 1994, 98, 1544.
- (10) Hunger, M.; Engelhardt, G.; Koller, H.; Weitkamp, J. Solid State Nucl. Magn. Reson. 1993, 2, 111.

- (11) Koller, H.; Burger, B.; Schneider, A. M.; Engelhardt, G.; Weitkamp, J. Microporous Mater. 1995, 5, 219.
- (12) Feuerstein, M.; Hunger, M.; Engelhardt, G.; Amoureux, J. P. Solid State Nucl. Magn. Reson. 1996, 7, 95.
- (13) Baker, M. D.; Ozin, G. A.; Godber, J. Catal. Rev. Sci. Eng. 1989, 27, 591.
- (14) Krause, K.; Geidel, E.; Kindler, J.; Förster, H.; Böhlig, H. J. Chem. Soc., Chem. Commun. 1995, 2481.
- (15) Jelinek, R.; Özkar, S.; Ozin, G. A. J. Phys. Chem. 1992, 96, 5949.
- (16) Jelinek, R.; Özkar, S.; Pastore, H. O.; Malek, A.; Ozin, G. A. J. Am. Chem. Soc. 1993, 115, 563.
- (17) Pastore, H. O.; Ozin, G. A.; Poë, A. J. J. Am. Chem. Soc. 1993, 115, 1215.
- (18) Brémard, C.; Ginested, G.; Laureyns, J.; Le Maire, M. J. Am. Chem. Soc. 1995, 117, 9274.
- (19) Özkar, S.; Ozin, G. A.; Moller, K.; Bein, T. J. Am. Chem. Soc. **1990**, 112, 9575.
- (20) Brémard, C.; Denneulin, E.; Depecker, C.; Legrand, P. Stud. Surf. Sci. Catal. 1989, 228.
- (21) Samoson, A.; Lippmaa, E. J. Magn. Reson., Ser. A 1989, 84, 410.
 (22) You-Sing, Y.; Howe, R. F. J. Chem. Soc., Faraday Trans. 1 1986, 82, 2887.

- (23) Medek, A.; Harwood, J. S.; Frydman, L. J. Am. Chem. Soc. 1995, 117, 12779.
 - (24) Koller, H.; Hunger, M.; Engelhardt, G. Unpublished results.
- (25) Klein, H.; Fuess, H.; Hunger, M. J. Chem. Soc., Faraday Trans. **1995**, *91*, 1813.
- (26) Jäger, C. NMR Basic Principles and Progress; Springer-Verlag: Berlin, 1994; Vol. 31, p 135.
- (27) Jacobs, W. P. J. H.; De Haan, J. W.; Van de Ven, L. J. M.; Van Santen, R. A. J. Phys. Chem. 1993, 97, 10394.
- (28) Mehring, M. High Resolution NMR Spectroscopy of Solids; Springer-Verlag: Berlin, 1976.
 - (29) Mason, J. Solid State Nucl. Magn. Reson. 1993, 2, 285.
 - (30) Gleeson, J. W.; Vaughan, R. W. J. Chem. Phys. 1983, 78, 5384.
- (31) Walter, T. H.; Thompson, A.; Keniry, M.; Shinoda, S.; Brown, T. L.; Gutowsky, H. S.; Oldfield, E. J. Am. Chem. Soc. 1988, 110, 1065.
- (32) Cybulski, P. A.; Gillis, D. J.; Baird, M. C. Inorg. Chem. 1993, 32, 460.
- (33) Koller, H.; Overweg, A. R.; Van de Ven, L. J. M.; De Haan, J. W.; Van Santen, R. A. In preparation.